Extended First-Principles Thermochemistry for the Oxidation of Titanium Tetrachloride

Philipp Buerger[a], Jethro Akroyd[a], Markus Kraft[a,b,*]

[a] *Department of Chemical Engineering and Biotechnology, University of Cambridge, West Cambridge Site, Philippa Fawcett Drive, Cambridge CB3 0AS, United Kingdom*
[b] *School of Chemical and Biomedical Engineering, Nanyang Technological University, 62 Nanyang Drive, Singapore, 637459*

Abstract

A detailed first-principles investigation of the gas-phase precursor chemistry of titanium tetrachloride ($TiCl_4$) in an O_2 environment is used to identify the thermodynamically most stable oxidation products. Candidate species are systematically proposed based on twelve manually defined base moieties in combination with possible functional groups attached to each moiety. The ground state geometry and vibrational frequencies for each candidate species are calculated using density functional theory at the B97-1/6-311+G(d,p) level of theory. A set of 2,328 unique candidate species are found to be physically reasonable. Their thermochemical data are calculated by applying statistical thermodynamics. Standard enthalpies of formation are estimated, if unknown, by using a set of error-cancelling balanced reactions. An equilibrium composition analysis of a mixture of $TiCl_4/O_2$ (50 mol%) at 3 bar is performed to identify the thermodynamically stable products. At low temperatures, below approximately 700 K, trimer species are dominant. This is followed by a mid-temperature range of 700 to 1975 K where Ti_2OCl_6 is the most abundant species, before its thermodynamic stability decreases. Between 1200 and 1825 K $TiCl_4$ is the most stable monomer. At temperatures above 1975 K $TiOCl_2$ becomes the dominant species. This species has been measured experimentally. A structural analysis

*Corresponding author
Email address: mk306@cam.ac.uk (Markus Kraft)

is used to suggest further potentially stable higher polymers and defines a starting point to investigate the mechanisms leading to the formation of titanium dioxide (TiO_2) particles.

Keywords: titanium dioxide, titanium tetrachloride, thermochemical data, thermochemistry calculations, electronic structure calculations, chemical equilibrium

1. Introduction

The manufacture of pigmentary titanium dioxide (TiO_2, titania) is a multi-billion dollar business. In 2015 the U.S. Geological Survey estimated the annual global TiO_2 pigment production capacity at 7.2 million metric tons [1].

The oxidation of $TiCl_4$, known as the chloride process [2, 3], is one of two major routes used for the commercial manufacture of TiO_2 particles. Purified $TiCl_4$ is oxidised in either a flame [4] or by stage-wise addition to an oxygen plasma [5, 6] at elevated pressure [7] to produce TiO_2 particles and chlorine. The overall stoichiometry of the process is described by

$$TiCl_4(g) + O_2(g) \longrightarrow TiO_2(s) + 2\,Cl_2(g). \quad (1)$$

Physical parameters such as size, shape, morphology and crystalline phase strongly influence the functional behaviour of the product particles and therefore their application. Improving the ability to control these properties is a key strategic capability. Various investigations have sought to develop an understanding of the underlying chemical and physical processes in an attempt to understand how to control the particle properties more efficiently.

Ghoshtagore [8] used chemical vapour deposition to investigate the surface reaction of $TiCl_4$ on single crystal silicon wafers with a TiO_2 film at 673–1120 K. The reaction was observed to display an Eley-Rideal dependence on $TiCl_4$ and O_2. The global kinetics of $TiCl_4$ oxidation in a hot wall reactor at 973–1273 K was studied by Pratsinis et al. [9]. The reaction was first-order in $TiCl_4$ and approximately zero-order in O_2 up to ten-fold excess O_2. Pratsinis and Spicer [10]

inferred a rate for the gas-phase decomposition of $TiCl_4$ based on the difference between the surface growth rate [8] and the global oxidation rate [9] under the assumption of monodisperse spherical particles. They showed that surface reaction had a significant effect on the particle diameter. Later studies using more detailed population balance models draw similar conclusions [11, 12, 13, 14].

West et al. [15, 16, 17] proposed the first detailed thermodynamically consistent gas-phase kinetic model to describe the oxidation of $TiCl_4$. This model consists of 20 $Ti_xO_yCl_z$ ($x \geq 1$, $y \geq 0$, $z \geq 0$) species which were defined based on the available literature and the authors' expertise. Oxychloride species were identified as important intermediates and the main reaction pathway was suggested to proceed via $Ti_2O_2Cl_4$. Thermochemical data were estimated by density functional theory (DFT) and statistical thermodynamics. Subsequent investigations presented an updated reaction mechanism [17] and considered the role of hydrocarbon species [18] and aluminium trichloride ($AlCl_3$) additives, known to promote the formation of the rutile crystal phase [19]. By analysing the combustion of $TiCl_4$ in a methane flame it was shown that the mole fraction of H-containing Ti-species is substantial at equilibrium and therefore likely to be important [18]. It was found that negligible quantities of Al-containing Ti-species were present at equilibrium. Consequently it was suggested that it is more likely that $AlCl_3$ acts via the particle processes to promote the formation of rutile TiO_2 particles [19].

A large number of modelling studies have assumed simplified reaction mechanisms and often a one-step mechanism [11, 20, 10, 21, 22]. In the work of Kraft and co-workers [23, 24] it was observed that the choice of inception mechanism strongly affects the simulations of Pratsinis' original experiment [9]. This is consistent with the work of Mehta et al. [25] who compared the inception behaviour of the mechanisms from Pratsinis and Spicer [10] (one-step mechanism) and West et al. [17] (detailed mechanism). They showed that the choice of inception model caused particle inception to occur at different locations in simulations of a turbulent flame. Recently Mehta et al. [26] proposed a reduced version of the West et al. [17] mechanism to describe the oxidation of

$TiCl_4$ in simulations of turbulent methane flames suitable to be coupled with computational fluid dynamics.

An accurate prediction of particle properties must consider the coupling between the gas- and particulate phase. In the absence of a full understanding of the gas-phase kinetics influencing the rate of nucleation and surface growth, significant approximations have to be made that affect the quality of the model, the level of predictability that should be expected from the results and our ability to understand the processes that control the properties of the particulate phase. A necessary step to improve the model is to develop a comprehensive description of the gas-phase chemistry.

The purpose of this work is to extend the work of West et al. [15] . Possible gas-phase species are systematically identified. The thermodynamic properties of the full species set are calculated at a consistent level of theory. The resulting thermodynamic properties are used to calculate the equilibrium composition to identify thermodynamically stable species. This defines a subset of species that should be considered when refining and extending the gas-phase kinetic model. Like West et al. [15], we focus on the industrial process where $TiCl_4$ reacts in a pure oxygen environment. For this reason, we calculate the equilibrium composition at 3 bar over a temperature range of $500 - 3000$ K, and we do not consider species that contain carbon or hydrogen. Subsequent steps (that are beyond the scope of the current work) would be to identify key intermediate species and reaction pathways, to calculate the corresponding reaction rates, and to couple the resulting gas-phase chemical mechanism to a population balance model describing the evolution of TiO_2 particles. Whilst the scope of the current work is limited to gas-phase species, the data provided with the manuscript provide a solid and necessary foundation for such work.

The rest of this paper is organised as follows. Section 2 describes the identification of candidate species. Sections 3 and 4 describe the calculation of the electronic structure and thermodynamic properties of the candidate species. Section 5 presents an equilibrium composition analysis and identifies key species. The results are critically assessed versus the findings of West et al. [15]. Sec-

tion 6 discusses mechanistic considerations in the light of the equilibrium analysis. Section 7 draws conclusions and makes closing remarks about next steps.

2. Candidate Species Generation

An algorithm was applied to systematically identify possible titanium-containing products created during the oxidation of $TiCl_4$. It makes use of a set of base moieties (molecules without their functional groups) in combination with possible functional groups to propose a set of candidate species.

2.1. Algorithm and Base Moieties

A set of titanium-containing base moieties is specified as input to the algorithm. The moieties contain sub-valent sites to which functional groups can be attached. The full set of moieties used in this work is shown in Figure 1. Species containing one titanium centre are addressed as monomers, those with two titanium centres as dimers and those with three titanium centres as trimers. Monomers with coordination numbers of four, five and six were considered. It was subsequently shown that that the impact of monomers with higher coordination numbers was minor and therefore only dimers and trimers with a coordination number of four were considered.

The algorithm systematically combines the moieties with possible functional groups to generate a set of candidate species. The functional groups $-$OCl, $-$O and $-$Cl as well as a possible sub-valent sites were considered in the algorithm. Duplicates were identified using a molecular representation, for example InChI [27, 28], SMILES [29, 30] or canonical SMILES [31, 30], and were rejected. An illustration of the algorithm for two different species is given in Figure 2.

In addition, $Ti_2O_2Cl_5$ (in this work labelled as $Ti_2O_2Cl_5{-}3$), $Ti_2O_2Cl_6$ (in this work labelled as $Ti_2O_2Cl_6{-}2$) and $Ti_5O_6Cl_8$ were considered by West et al. [15, 17] and were included in the set of candidate species for the purpose of comparison.

The effect of spin multiplicity on the ground states of the titanium-containing species derived from titanium tetraisopropoxide (TTIP, $Ti(OC_3H_7)_4$) [32] was

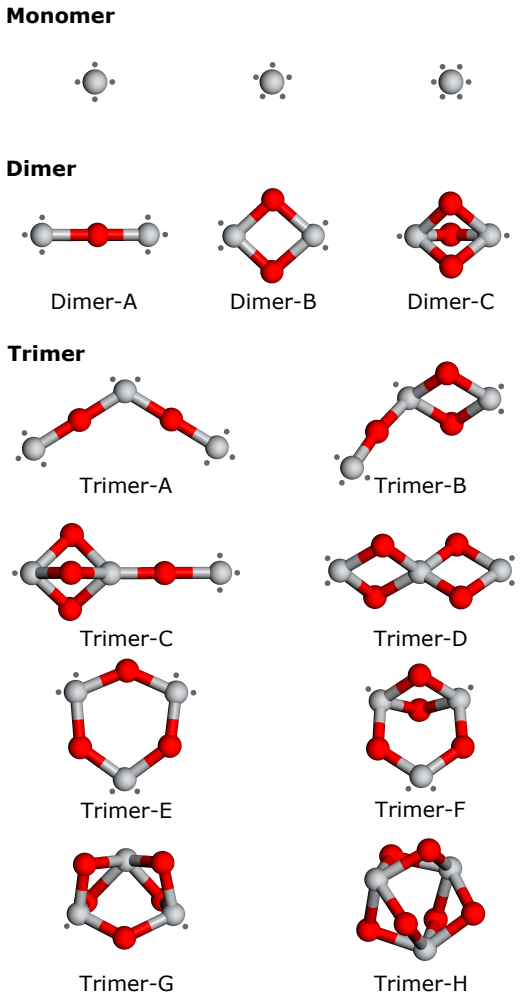

Figure 1: Manually defined base moieties for possible products which could be present during the titanium tetrachloride ($TiCl_4$) oxidation. These moieties consist of atomic titanium (grey), oxygen (red) and sub-valent sites (.). Functional groups are able to be attached to the sub-valent sites.

analysed. It was observed that bonds between two $-O$ groups can increase the stability of a species as illustrated in Figure 3. The algorithm automatically identifies the combinations of functional groups that could lead to such intramolecular interactions and a separate candidate species is generated for each such case. The original species without any functional group interactions

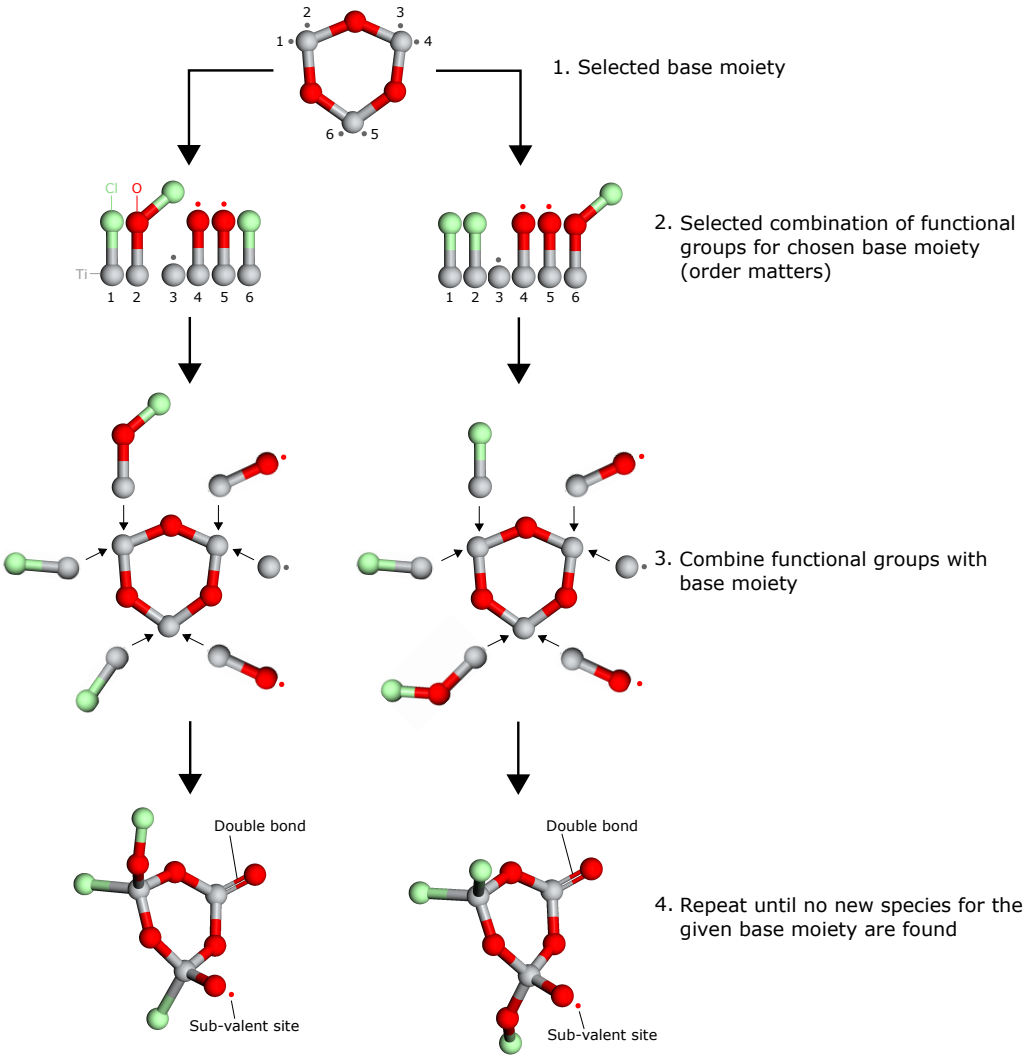

Figure 2: Principle of the species generation algorithm used to systematically generate possible titanium tetrachloride ($TiCl_4$) oxidation products. The algorithm is illustrated for a selected base moiety and two combinations of functional groups.

also remains within the set. In this work only O−O interactions were considered.

The structural families in this paper are defined by classifying each candidate species by its base moiety. For example, all species containing two titanium atoms connected by two oxygen atoms is a member of the structural family Dimer-B.

(a) No intramolecular interaction.

(b) With intramolecular interaction.

Figure 3: Illustrative example of a possible intramolecular interaction between the two −O groups.

2.2. Results

An initial set of 119,148 $Ti_kO_lCl_m$ ($1 \leq k \leq 3$, $l \geq 0$, $m \geq 0$) species was generated, of which 5,543 unique species remained after rejecting duplicates. In order to keep the set at a manageable size, species with more than three Ti atoms (other than the $Ti_5O_6Cl_8$ pentamer considered by West et al. [15]) were not considered due to the combinatorial increase in the number of species.

It was assumed that species with more than one radical site are likely to be short-lived. Trimers with more than one radical site were rejected under the assumption that they are unlikely to be thermodynamically stable and are therefore unlikely to play an important role in the equilibrium composition analysis. Radical monomers and dimers with more than one radical site were kept on the basis that the resulting thermochemistry data may be important for future refinement of the kinetic mechanism and that the number of these species was small enough for this to be feasible. This reduced the set of candidate species to a total of 2,436 unique species.

3. Electronic Structure Calculations

3.1. Geometry Optimisations and Frequency Calculations

Geometry optimisation and frequency calculations were performed using density functional theory (DFT) at the B97-1/6-311+G(d,p) level of theory for each of the 2,436 candidate species. All species in the current work were

neutrally charged. The B97-1 hybrid functional has been shown to be accurate [33, 34] and well suited for transition metal complexes [35, 36, 37, 38], including titanium-containing species in the context of the thermal oxidation of $TiCl_4$ [38]. Scaling factors were used as proposed by Merrick et al. [39] to compensate for the overestimation of the calculated harmonic frequencies.

The Gaussian09 software package [40], running on Intel(R) Xeon(R) CPU X5472 @ 3.00GHz / 8GB nodes with 8 cores per node, was used to perform all electronic structure calculations. A tight convergence criterion and an ultrafine (99,590) pruned grid were chosen. The calculations were set to distinguish between open- and closed-shell species. Analysing the effect of the spin multiplicity on the calculated ground states of species derived from TTIP [32] showed that it was valid to select the spin multiplicity based on the number of sub-valent sites for each species. Besides the restricted DFT calculations, unrestricted computations were performed for the set of closed-shell species in order to investigate the effect of spin contamination.

The initial guess of the geometry for each candidate species was extracted from the optimised ground state geometry of the largest species in the structural family. In this work, the largest species is formed from the base moiety with only the $-OCl$ functional groups attached. These species were optimised stepwise, building the molecule atom-by-atom from the base moiety, re-optimising the structure after adding each layer of new atoms. This reduced the overall optimisation problem to a set of smaller problems. Each optimisation step was started from a near-optimal geometry with the aim of increasing the likelihood of finding the global minimum. In addition, the ground state geometries of multiple conformers were calculated in the case of species showing high degrees of freedom. This mainly included candidate species of the families Dimer-A and Trimer-A. Also in cases were the geometry optimisation failed to converge, multiple manually defined geometries were used as initial guesses.

This approach to calculating the ground state geometry was developed in previous work [32], where it was shown that the algorithm was robust to the problem of conformers, providing a basis to be confident about the current work.

In several cases, initially distinct candidate species converged to the same structure. The duplicates were identified using canonical SMILES as implemented in OpenBabel [30] and were removed from the species set. Only the lowest energy conformer was retained.

3.2. Results

The ground state geometries and vibrational frequencies were calculated for all candidate species. It was verified that no imaginary frequencies were present. The optimised ground state geometries of key species are presented in Figure 4. The calculated ground state energies of restricted and unrestricted DFT computations for closed-shell species were consistent.

It was observed that some structural families seem to be more physically reasonable than others. For example, the convergence of an initial Dimer-A type geometry into a Dimer-B type geometry, indicating that double oxygen bridges are favoured over radical oxygen groups. Another observation was that the cyclic structures (Trimer-E and Trimer-F) seemed to be more reasonable than the non-cyclic ones. In particular Trimer-A and Trimer-B type species often converged into more compact cyclic or bent unclosed-cyclic structures.

After removing duplicates, the final set of candidate species with optimised ground state geometries and calculated scaled frequencies consisted of $2,328$ unique titanium-containing species.

4. Thermochemistry Calculations

4.1. Partition Functions

Statistical thermodynamics was used to calculate the heat capacity, entropy and enthalpy of each species for the temperature range $200 - 4000$ K. Translational, vibrational, rotational and electronic energy contributions were considered. The standard classical approximation was used for the treatment of the translational and rotational motion. A simple harmonic-oscillator approximation was used to approximate the effect of the vibrational motions. The effect

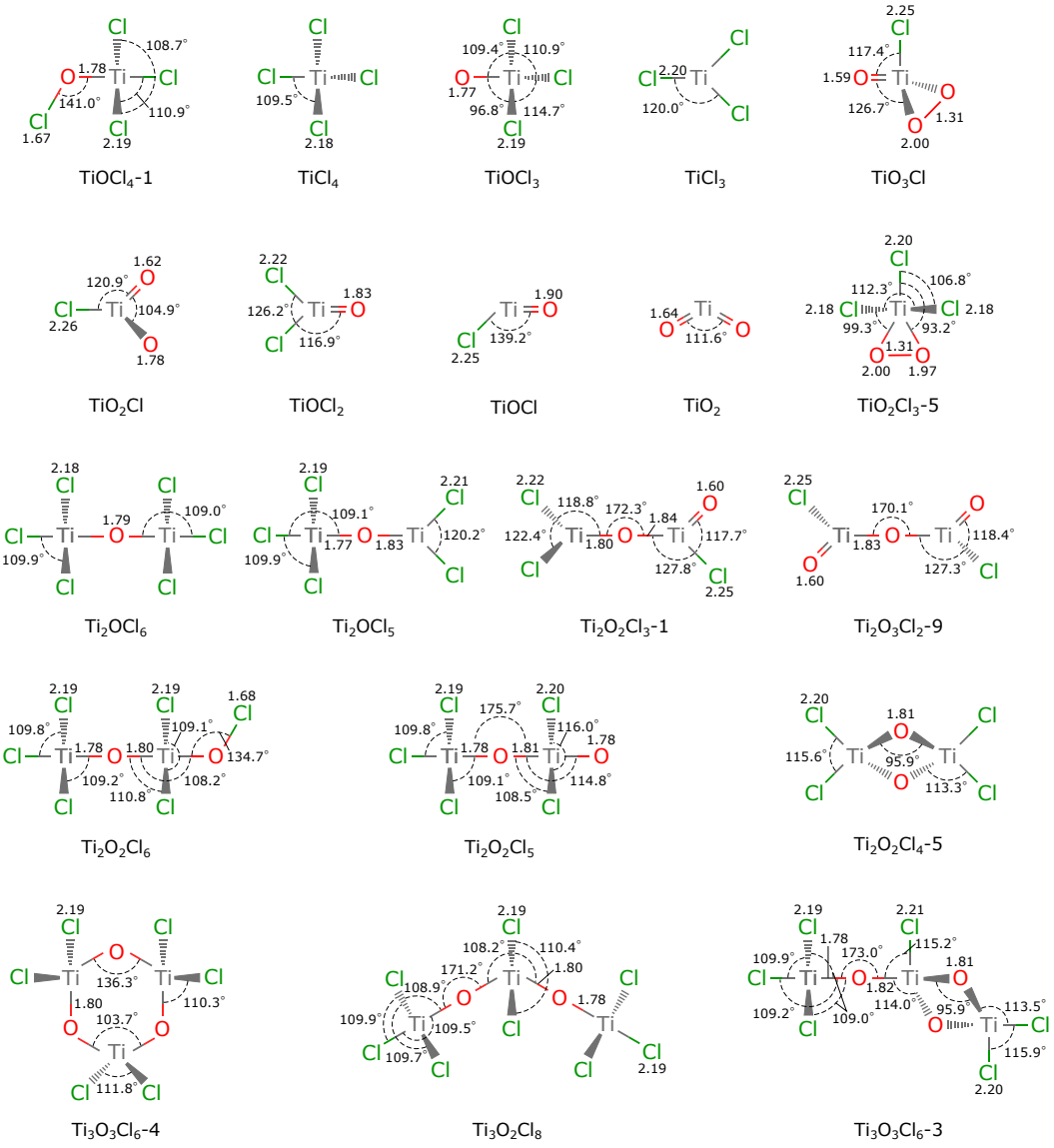

Figure 4: Optimised ground state geometries for key species calculated at the B97-1/6-311+G(d,p) level of theory. Bond lengths are reported in Ångströms.

of considering hindered rotors was investigated in our previous work [32], where it was shown that the detailed treatment of internal rotations had a negligible impact on the calculated equilibrium composition, and that a simple rigid-rotor

harmonic oscillator (RRHO) approximation, without the explicit consideration of internal rotations, was sufficient for the identification of important thermodynamically stable products [32]. It was assumed that only the ground state is accessible, which reduces contributions from the electronic mode to the spin multiplicity (1 for non-radical species). Details about partition function calculations can be found in a number of textbooks [41, 42].

The calculation method has previously been validated against hydrocarbons and showed very good agreement with available experimental data [32]. Molecular symmetry numbers were determined using the Jmol software package [43].

4.2. Enthalpy Correction

The partition functions allow for the calculation of the enthalpy change,

$$\Delta H(T) = H(T) - H(0\ \mathrm{K}), \tag{2}$$

where $H(T)$ is the absolute enthalpy at temperature T. In order to calculate the absolute enthalpy $H^\circ(T)$ it is necessary to calculate $H^\circ(0\ \mathrm{K})$, which is equal to the standard enthalpy of formation at 0 K $\Delta_\mathrm{f}H^\circ_{0\ \mathrm{K}}$. Assuming a temperature of 298.15 K, Equation (2) can be rewritten as,

$$\Delta H^\circ(298.15\ \mathrm{K}) = \Delta_\mathrm{f}H^\circ_{298.15\ \mathrm{K}} - \Delta_\mathrm{f}H^\circ_{0\ \mathrm{K}}. \tag{3}$$

Given the standard enthalpy of formation, $\Delta_\mathrm{f}H^\circ_{298.15\ \mathrm{K}}$, and the enthalpy change, $\Delta_\mathrm{f}H^\circ_{298.15\ \mathrm{K}}$, at 298.15 K, Equation (3) can be solved for $\Delta_\mathrm{f}H^\circ_{0\ \mathrm{K}}$ and Equation (2) for $H^\circ(T)$.

The standard enthalpy of formation is not always known experimentally or theoretically. In the case of species where data was not available, the concept of error-cancelling balanced reactions (EBRs) was used to obtain an estimate of the standard enthalpy of formation. By applying Hess' law, the enthalpy of formation of one of the species in an EBR can be calculated based on knowledge of the enthalpies of formation of the other species in the reaction. This method requires knowledge of the total energy for each species in the EBR and the

standard enthalpies of formation for all except the species for which the enthalpy is being calculated.

The *isodesmic* and *isogyric* reaction classes were used in this work [44, 45, 46]. Isogyric reactions conserve the number of spin pairs, whilst isodesmic reactions conserve the bond types between two atoms on either side of the reaction, such that systematic errors inherited from the electronic structure calculations approximately cancel out. The choice of the reaction has an effect on the accuracy of the estimate of the standard enthalpy of formation. For this reason, an automatically identified set of EBRs was used to derive a distribution of possible standard enthalpy of formation values from which an average value of the enthalpy of formation was calculated. This has been shown to significantly improve the accuracy of the method and to additionally provide an estimate of the statistical uncertainty in the results. The width of the distribution, in form of the empirical standard deviation, was used to define the statistical uncertainty. This methodology has been extensively tested and validated for test data sets including carbon, hydrogen, oxygen, chlorine and titanium [47, 48].

The reference data for the standard enthalpies of formation used in this work are listed in Table 1. Absolute differences between literature data of up to 94 kJ mol^{-1} were found for the oxychloride species. The effect of the reference data (Table 1) on the accuracy of the method was assessed using a cross-validation technique. The method was described in full elsewhere [47, 48] and is only summarised here. The standard enthalpy of formation was iteratively estimated for each species in the reference set, assuming that the enthalpy of the species under investigation is unknown. The estimated value was then compared against the reference value and an accuracy metric assigned to the data. The cross-validation was used to identify and avoid the use of unreliable and inconsistent reference data. The data in Table 1 are the final post cross-validation reference data that were used in this work.

Table 1: Reference data for standard enthalpies of formation for relevant species.

species	$\Delta_f H^\circ_{298.15\ \mathrm{K}}$ [kJ mol^{-1}]	species	$\Delta_f H^\circ_{298.15\ \mathrm{K}}$ [kJ mol^{-1}]
Ti−Cl species		*Other species*	
$TiCl_4$	−763 [49, 50]	ClO	102 [49, 50, 51, 52, 53]
$TiCl_3$	−508 [54]	ClO_2	98 [49, 50]
$TiCl_2$	−205 [54]	ClO_3	201 [55]
TiCl	171 [54]	ClO_4	229 [56]
		OClO	95 [49, 50, 53, 57, 58]
Ti−O−Cl species		Cl_2	0 [49, 50]
$TiOCl_2$	−593 [59]	ClOCl	83 [51]
TiOCl	−287 [48]	Cl_2O	90 [49, 50]
		$ClClO_2$	154 [49, 50, 60, 61]
Ti−O species		Cl_2O_3	137 [51]
TiO_2	−305 [49, 50]	Cl_2O_4	186 [62]
TiO	54 [49, 50]	Cl_2O_5	258 [62]
		Cl_2O_6	279 [62]
		Cl_2O_7	321 [62]
		ClOClO	176 [49, 50, 61]
		ClOOCl	133 [51]
		O_2	0 [49, 50]

4.3. Results

4.3.1. Cross-Validation of the Enthalpy of Formation

The cross-validation of the reference species (Table 1) was performed separately using isodesmic and isogyric reactions. A mean absolute error of 12 kJ mol^{-1} was observed using isodesmic reactions and 48 kJ mol^{-1} using isogyric reactions. In addition, the mean absolute error was also calculated separately for titanium-containing species. The mean absolute error for titanium-containing species was 3 kJ mol^{-1} for isodesmic reactions and 20 kJ mol^{-1} for isogyric reactions.

The larger error for isogyric reactions was not unexpected because this reaction class is far less restrictive than isodesmic reactions. These errors are expected given the differences in literature data (for example up to 94 kJ mol^{-1} for the oxychloride species) and the corresponding reference data that are used in the calculations (Table 1).

4.3.2. Calculation of the Enthalpy of Formation

The enthalpy of formation of the candidate species was calculated using isodesmic reactions wherever possible. However, the small number of species for which reference data was available, meant that isogyric reactions had to suffice for most species. A larger set of titanium-containing reference species would enable the use of more isodesmic reactions and lead to lower uncertainties in the estimated standard enthalpies.

The calculations in this work did not rely on a single EBR, but used a set of EBRs for each species. This has been shown to significantly improve the accuracy of calculations based on EBRs [47, 48], providing some compensation from the use of isogyric reactions.

The largest discrepancy between the enthalpy estimates of West et al. [15] and those calculated here is for TiO_2Cl_2. A set of 17 isogyric reactions was used to estimate a standard enthalpy of formation of -627 ± 19 kJ mol^{-1} compared to -558 kJ mol^{-1} for TiO_2Cl_2. None of the calculated isogyric reactions for TiO_2Cl_2 were close to the value of -558 kJ mol^{-1} [15], which was estimated using a single anisogyric reaction. The closest and largest value for TiO_2Cl_2 observed within the distribution was -590 kJ mol^{-1}. For all other species considered by West et al. [15, 17], the enthalpy estimates are in acceptable agreement with those calculated in this work.

4.3.3. Thermochemistry

The calculated thermochemical data are in excellent agreement with those proposed by West et al. [15]. Thermochemical data for key titanium-containing species are reported in Table 2. In addition, the calculated thermochemical data for the full set of candidate species are provided as supporting information.

Table 2: Thermochemical data for $TiCl_4$ and selected oxidation products. Where available, reference data for the standard enthalpies of formation were taken from the literature.

species	$\Delta_f H^\circ_{298.15\ K}$	$S^\circ_{298.15\ K}$	C_P° [J mol^{-1} K^{-1}]						
	[kJ mol^{-1}]	[J mol^{-1} K^{-1}]	300	500	1000	1500	2000	2500	3000
Monomer									
$TiCl_4$	-763 [50, 49]	355.66	96.17	103.43	106.82	107.51	107.78	107.87	107.94
$TiOCl_4$−1	-759	422.66	114.43	124.68	130.61	131.92	132.43	132.62	132.73
$TiCl_3$	-508 [54]	340.24	75.27	80.07	82.30	82.76	82.94	83	83.04
$TiOCl_3$	-635 [a]	375.51	95.01	102.6	106.59	107.41	107.73	107.84	107.91
TiO_2Cl_3−5	-781 [b]	402.17	111.01	122.32	129.69	131.47	132.18	132.44	132.61
$TiOCl_2$	-593 [59]	337.51	70.31	76.53	81.08	82.18	82.62	82.78	82.88
TiOCl	-287 [48] [c]	292.45	49.34	53.34	56.66	57.48	57.81	57.93	58.01
TiO_2Cl	-493	318.34	70.23	76.84	81.26	82.27	82.67	82.82	82.91
TiO_3Cl	-673	340.24	83.58	94.78	103.79	106.06	106.97	107.32	107.54
TiO_2 [e]	-305 [50, 49]	258.69	43.54	49.87	55.56	56.96	57.52	57.73	57.87
Dimer									
Ti_2OCl_6	-1587	562.33	180.56	196.41	204.64	206.39	207.08	207.32	207.47
$Ti_2O_2Cl_6$	-1593	609.58	198.78	217.72	228.48	230.82	231.74	232.06	232.27
Ti_2OCl_5	-1334	543.83	159.78	173.09	180.14	181.65	182.24	182.45	182.58
$Ti_2O_2Cl_5$	-1471	571.99	179.30	195.64	204.41	206.29	207.02	207.27	207.44
$Ti_2O_2Cl_4$−5	-1541 [d]	451.87	149.84	168.50	178.86	181.06	181.92	182.23	182.42
$Ti_2O_2Cl_3$−1	-1167	501.18	133.73	146.14	154.40	156.32	157.08	157.35	157.53
$Ti_2O_3Cl_2$−9	-1218	471.20	128.39	142.51	153.17	155.73	156.75	157.13	157.37
Trimer									
$Ti_3O_3Cl_6$−3	-2362	657.17	234.08	261.43	276.67	279.94	281.21	281.66	281.96
$Ti_3O_3Cl_6$−4	-2427	607.87	235.31	262.23	276.90	280.05	281.27	281.71	281.99
$Ti_3O_2Cl_8$	-2411	740.58	264.80	289.38	302.47	305.28	306.37	306.76	307.01

[a] West et al. [15] reported a value of −639 kJ mol^{-1}.

[b] West et al. [15] reported a value of −774 kJ mol^{-1}.

[c] West et al. [15] reported a value of −274 kJ mol^{-1}.

[d] West et al. [15] reported a value of −1552 kJ mol^{-1}.

[e] Literature data taken from the database provided with Cantera [63, 64] and originating from the NASA thermochemical database [65].

5. Equilibrium Composition Analysis

Equilibrium composition analysis was used to identify the thermodynamically stable $TiCl_4$ oxidation products. In this work the thermodynamic stability is defined by the relative mole fractions of each compound. Figure 5 presents the calculated equilibrium composition for an initial mixture of $TiCl_4/O_2$ (50 mol%) at 3 bar, similar to those in an industrial reactor, for a temperature range of $500 - 3000$ K, where each point on the graph was calculated at constant pressure and temperature. The full set of $2,328$ $Ti_kO_lCl_m$ candidate species plus 20 O_lCl_m ($l \geq 0$, $m \geq 0$) species were included in the calculation. The equilibrium composition was calculated using Cantera [63, 64]. The thermochemical data for O, O_2, O_3, Cl, Cl_2, Ti, TiO and TiO_2 were taken from the database provided with Cantera [63, 64] and originated from the NASA thermochemical database [65]. Thermochemical data for all other species considered in this work were calculated as per Sections 3 and 4.

The titanium-containing species in Figure 5 are all present at high mole fractions. This includes $TiOCl_2$, Ti_2OCl_6, $Ti_3O_3Cl_6$−4, $TiCl_4$, $Ti_3O_2Cl_8$, $Ti_3O_3Cl_6$−3, $Ti_2O_2Cl_4$−5, TiOCl, TiO_2Cl, $TiCl_3$, $Ti_2O_2Cl_3$−1, $Ti_2O_3Cl_2$−9, $TiOCl_4$−1, TiO_2, $Ti_2O_2Cl_6$, $Ti_2O_2Cl_5$, TiO_3Cl, $TiOCl_3$, TiO_2Cl_3−5 and Ti_2OCl_5. The optimised ground state geometries for these species are shown in Figure 4.

Trimer species are found to be most stable at low temperatures, below approximately 700 K. The main trimer species are $Ti_3O_3Cl_6$−4 and $Ti_3O_2Cl_8$. These are both non-radical species where the titanium atoms are connected by single oxygen atoms (single oxygen bridges). The single-radical trimer species are found to have low equilibrium mole fractions (none are visible in Figure 5). Trimer species with more radical sites are expected to be less stable than single-radical trimer species. This remains consistent with the decision to exclude trimers with more than one radical site from the analysis.

Above 700 K, the Ti_2OCl_6 dimer becomes dominant up to 1975 K. This also contains a single oxygen bridge. In addition, there are stable species with titanium atoms connected by two oxygen atoms (double oxygen bridges) in this

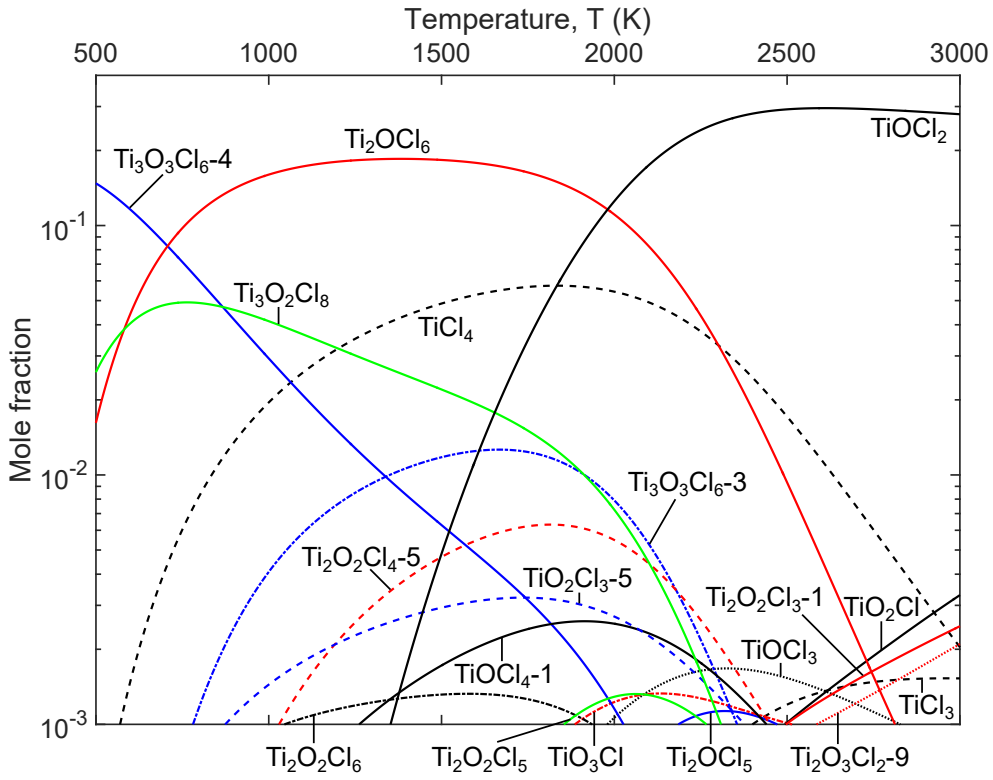

Figure 5: Calculated equilibrium composition as a function of temperature for an initial mixture of $TiCl_4/O_2$ (50 mol%) at 3 bar. Only titanium-containing species are shown. Optimised ground state geometries for these species are presented in Figure 4.

temperature range. This includes $Ti_2O_2Cl_4$−5 and $Ti_3O_3Cl_6$−3. A rapid increase in the thermodynamic stability of $TiOCl_2$ is observed above 1400 K. This species has also been observed experimentally [66] and becomes the most thermodynamically stable species above 1975 K. The $TiCl_4$ precursor is present at notable mole fractions at temperatures between 1200 and 1825 K. Its thermodynamic stability significantly decreases at high temperatures. The geometries of all of these species are shown in Figure 4. Only low mole fractions of the dimers $Ti_2O_2Cl_6$−2 (labelled $Ti_2O_2Cl_6$ by West et al. [17]) and $Ti_2O_2Cl_5$−3 (labelled $Ti_2O_2Cl_5$ by West et al. [17]), which possess titanium atoms with coordination numbers of five, were observed. Across the full temperature range,

other monomers with a coordination number of five or six were not stable.

The mole fractions of radical species such as TiOCl or TiO_2Cl are observed to increase with increasing temperature. Out of the species shown in Figure 5 only $TiOCl_4{-}1$ and $Ti_2O_2Cl_6$ were found to have an OCl functional group. Across all candidate species it was observed that the thermodynamically more stable species typically have fewer $-$OCl functional groups.

The systematic extension of the species set enables an assessment of whether any stable species were missing from the set proposed by West et al. [15]. Overall, a significant degree of agreement is found with the equilibrium composition calculated by West et al. [15], where species such as $TiOCl_2$, $TiCl_4$, TiO_2Cl_3 (in this work labelled as $TiO_2Cl_3{-}5$) and $Ti_2O_2Cl_4$ (in this work labelled as $Ti_2O_2Cl_4{-}5$) were found to be stable. Some differences are observed where West et al. [15] truncated the species set. For example, the mole fractions of the single trimer $Ti_3O_4Cl_4$ (in this work labelled as $Ti_3O_4Cl_4{-}6$) and pentamer $Ti_5O_6Cl_8$ considered by West et al. [15] were found to be significantly lower in this work. Such differences are to be expected because the species considered in the current work are a significant superset[1] of the titanium-containing species considered by West et al. [15].

Figure 6a summarises the equilibrium data in terms of monomers, dimers and trimers. As expected, larger polymers (trimers) are found to be thermodynamically most stable at lower temperatures below 700 K and their stability decreases with increasing temperature. It is observed that dimers are the thermodynamically most stable species group at temperatures between approximately 700 and 1975 K. The thermodynamic stability of monomers gradually increases with temperature and they are dominant at temperatures above approximately 1975 K.

Figure 6b shows the species mole fractions grouped by their structural family (Figure 1). The most abundant structural family at temperatures below 700 K

[1] 120 monomers, 366 dimers, 1,841 trimers and the $Ti_5O_6Cl_8$ pentamer versus 18 titanium-containing species considered by West et al. [15].

is Trimer-E. This contains cyclic species with single oxygen bridges. A rapid decrease in the thermodynamic stability of Trimer-E species is observed with increasing temperature. The Trimer-A and Trimer-B families are also observed at significant mole fractions. Both contain non-cyclic species. Trimer-A species contains single oxygen bridges. Trimer-B species contain both a single and double oxygen bridge. The Dimer-A family is dominant at temperatures between 700 and 1975 K. This contains species with single oxygen bridges. The Dimer-B family is also observed but at lower mole fractions. Over the full temperature range, Dimer-A was found to be thermodynamically more stable than Dimer-B. At temperatures above 1975 K, monomer species are most stable.

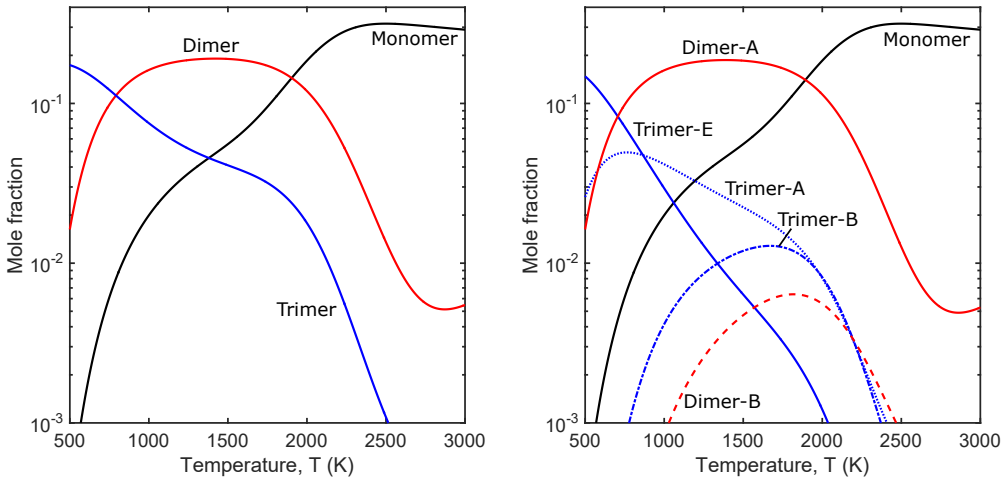

(a) Grouped species as monomers, dimers and trimers.

(b) Structural families as defined in Figure 1.

Figure 6: Summary of species groups for $TiCl_4$ oxidation products.

The structural analysis is useful to suggest further potentially stable higher polymers, whilst keeping the set of candidate species at a manageable size, rather than considering a combinatorially increasing number of species. This provides a starting point to investigate the mechanisms leading to the formation of TiO_2 particles.

6. Mechanistic Considerations

It is possible to gain some mechanistic insight based on the equilibrium composition analysis, presented in Section 5, and the existing reaction mechanism [16, 17].

Ti_2OCl_6 could be the product of a bimolecular reaction between $TiCl_3$ and $TiOCl_3$. Other pathways producing Ti_2OCl_6 are also possible and would need to be considered. In the mechanism proposed by West et al. [16, 17], $TiOCl_3$ is an essential intermediate on pathways to TiO_2Cl_4−5. It is assumed that $TiOCl_3$ may also be an important intermediate on pathways involving Ti_2OCl_6.

Depending on the temperature, $Ti_3O_2Cl_8$ could perhaps be involved in pathways that include Ti_2OCl_6 and $TiOCl_3$, $Ti_2O_2Cl_5$ and $TiCl_3$, and Ti_2OCl_5 and $TiOCl_3$. The abstraction of a chlorine atom from $Ti_2O_2Cl_5$ followed by an internal restructuring could lead to $Ti_2O_2Cl_4$−5. A similar internal restructuring of $Ti_2O_2Cl_5$ might also produce $Ti_2O_2Cl_5$−3. Both $Ti_2O_2Cl_4$−5 and $Ti_2O_2Cl_5$−3 were found to be important and are discussed in detail by West et al. [15, 16, 17].

This is certainly not a complete list and is not the focus of this work. Many other pathways may need to be considered. Likewise, many intermediate species are not thermodynamically stable, yet will play a critical role in the reaction mechanism. One way to approach this problem systematically could be to define reaction rules for the functional groups in each structural family. This would enable the automatic generation of an initial mechanism, similar to previous investigations of tetraethoxysilane (TEOS) [67] and titanium tetraisopropoxide (TTIP) [68]. The mechanism could then be refined iteratively.

7. Conclusions

An extended first-principles investigation of the gas-phase precursor chemistry of $TiCl_4$ in an O_2 environment was conducted using quantum chemistry, statistical thermodynamics and equilibrium composition analysis. A simple rigid-rotor harmonic-oscillator approximation was assumed. Thermochemical data for a large set of possible Ti−O−Cl species were calculated and analysed.

Possible candidate species, which could be present during the reaction of $TiCl_4$, were systematically identified. Species with up to three titanium atoms were considered, including monomer species with coordination numbers of four, five and six. Trimer species with more than one radical site were assumed to be short-lived and excluded from further analysis. Monomers and dimers with multiple radical sites were assumed to be important in the initial stages of the precursor chemistry, even though they might not be thermodynamically stable, and were kept in the species pool. The algorithm used to identify the species could be extended to other polymer species following the same geometric principles. The ground state geometry and scaled harmonic vibrational frequencies were calculated using the B97-1/6-311+G(d,p) level of theory for $2,328$ unique titanium-containing candidate species.

In cases where no standard enthalpy of formation was known, an automatically identified set of error-cancelling balanced reactions was used to calculate an informed estimate. Isodesmic reactions were preferentially used over isogyric reactions. It was found that due to the scarcity of reference data for titanium-containing species, the application of isodesmic reactions was limited and isogyric reactions had to suffice for most species. Acceptable mean absolute errors were calculated by performing a cross-validation for the titanium-containing species using each reaction class. Significant uncertainties in the calculated standard enthalpies of formation were shown to result from the necessary use of isogyric reactions and the limited set of error-cancelling balanced reactions that can be found given a small set of reference species. Additional experimental data would be beneficial in enabling the use of a wider range of balanced reaction and therefore in achieving higher accuracy estimates.

Equilibrium analysis was used to identify the thermodynamically stable titanium-containing species for an initial mixture of $TiCl_4/O_2$ (50 mol%) at 3 bar. Trimer species were found to be dominant at temperatures below 700 K. A mixture of trimers, dimers and monomers were stable between 700 to 2500 K. Ti_2OCl_6 was the most stable species between 700 and 1975 K, after which its stability decreased rapidly. At temperatures above 1975 K, $TiOCl_2$ became the

dominant species.

The equilibrium composition was analysed in terms of the structural families of the species. Trimer species including both cyclic and non-cyclic structures were dominant at low temperatures. Their stability decreased with temperature. At mid-temperatures, a mixture of structural families were present. This includes trimers, dimers with a single and double oxygen bridge and monomers. The Dimer-A family (single oxygen bridge) was prevalent over the Dimer-B family (double oxygen bridge) across the full temperature range. At temperatures above 1975 K, monomers were the most stable family.

The obvious next step would be to use these observations and the thermochemical data set generated in this work to refine the existing gas-phase chemical mechanism leading to the formation of particles. This will require the identification of reaction pathways, using the identified thermodynamically stable species as guide. An automated reaction mechanism generator could be employed to suggest possible pathways. Reaction rules could be defined based on structural families and attached functional groups. Thermochemical data for key species could be further refined by considering internal rotational motion to improve the quality of the reaction mechanism.

Acknowledgements

This project is partly funded by the National Research Foundation (NRF), Prime Minister's Office, Singapore under its Campus for Research Excellence and Technological Enterprise (CREATE) programme, and by the European Union Horizon 2020 Research and Innovation Programme under grant agreement 646121. The authors thank Huntsman Pigments and Additives for financial support.

Supplemental Material

Thermochemical data for the 2,328 candidate species are provided in the form of NASA polynomial coefficients in CHEMKIN format and as comma

separated (.csv) files tabulating the heat capacity, entropy and absolute enthalpy as a function of temperature. A table mapping each species to a SMILES string is also provided. The molecular geometries are available on request.

References

[1] U.S. Department of the Interior, U.S. Geological Survey, National Minerals Information Center, URL http://minerals.usgs.gov/minerals/, retrieved August 29, 2016, 2016.

[2] H. H. Schaumann, Production of Titanium Oxide Pigments, US Patent 2,488,439, 1949.

[3] I. J. Krchma, H. H. Schaumann, Production of Titanium Dioxide, US Patent 2,559,638, 1951.

[4] S. E. Pratsinis, S. Vemury, G. P. Fotou, A. Gutsch, Process for producing ceramic powders, especially titanium dioxide useful as a photocatalyst, U.S. Patent 5,698,177, URL http://www.google.com/patents/?id=OgwfAAAAEBAJ, 1997.

[5] A. J. Morris, M. D. Coe, System for increasing the capacity of a titanium dioxide producing process, U.S. Patent 4,803,056, URL http://www.google.com/patents/?id=R805AAAAEBAJ, 1989.

[6] J. C. Deberry, M. Robinson, M. D. Pomponi, A. J. Beach, Y. Xiong, K. Akhtar, Controlled vapor phase oxidation of titanium tetrachloride to manufacture titanium dioxide, U.S. Patent 6,387,347 B1, URL http://www.google.com/patents/?id=r3gKAAAAEBAJ, 2002.

[7] A. J. Haddow, Oxidation of titanium tetrachloride to form titanium dioxide, U.S. Patent 5,599,519, URL http://www.google.com/patents/?id=8WMdAAAAEBAJ, 1997.

[8] R. N. Ghoshtagore, Mechanism of Heterogeneous Deposition of Thin Film Rutile, J. Electrochem. Soc. 117 (4) (1970) 529–34, doi:10.1149/1.2407561.

[9] S. E. Pratsinis, H. Bai, P. Biswas, M. Frenklach, S. V. R. Mastrangelo, Kinetics of Titanium(IV) Chloride Oxidation, J. Am. Ceram. Soc. 73 (7) (1990) 2158–62, doi:10.1111/j.1151-2916.1990.tb05295.x.

[10] S. E. Pratsinis, P. T. Spicer, Competition Between Gas Phase and Surface Oxidation of $TiCl_4$ During Synthesis of TiO_2 Particles, Chem. Eng. Sci. 53 (10) (1998) 1861–8, doi:10.1016/S0009-2509(98)00026-8.

[11] S. Tsantilis, S. E. Pratsinis, Narrowing the Size Distribution of Aerosol-Made Titania by Surface Growth and Coagulation, J. Aerosol Sci. 35 (3) (2004) 405–20, doi:10.1016/j.jaerosci.2003.09.006.

[12] N. Morgan, C. Wells, M. Kraft, W. Wagner, Modelling Nanoparticle Dynamics: Coagulation, Sintering, Particle Inception and Surface Growth, Combust. Theor. Model. 9 (3) (2005) 449–61, doi:10.1080/13647830500277183.

[13] N. Morgan, C. G. Wells, M. J. Goodson, M. Kraft, W. Wagner, A New Numerical Approach for the Simulation of the Growth of Inorganic Nanoparticles, J. Comput. Phys. 211 (23) (2006) 638–58, doi:10.1016/j.jcp.2005.04.027.

[14] M. C. Heine, S. E. Pratsinis, Polydispersity of Primary Particles in Agglomerates Made by Coagulation and Sintering, J. Aerosol Sci. 38 (1) (2007) 17–38, doi:10.1016/j.jaerosci.2006.09.005.

[15] R. H. West, G. J. O. Beran, W. H. Green, M. Kraft, First-Principles Thermochemistry for the Production of TiO_2 from $TiCl_4$, J. Phys. Chem. A 111 (18) (2007) 3560–5, doi:10.1021/jp0661950.

[16] R. H. West, M. S. Celnik, O. R. Inderwildi, M. Kraft, G. J. O. Beran, W. H. Green, Toward a Comprehensive Model of the Synthesis of TiO_2 Particles from $TiCl_4$, Ind. Eng. Chem. Res. 46 (19) (2007) 6147–56, doi:10.1021/ie0706414.

[17] R. H. West, R. A. Shirley, M. Kraft, C. F. Goldsmith, W. H. Green, A Detailed Kinetic Model for Combustion Synthesis of Titania from $TiCl_4$, Combust. Flame 156 (9) (2009) 1764–70, doi:10.1016/j.combustflame.2009.04.011.

[18] T. S. Totton, R. Shirley, M. Kraft, First-Principles Thermochemistry for the Combustion of $TiCl_4$ in a Methane Flame, Proc. Combust. Inst. 33 (1) (2011) 493–500, doi:10.1016/j.proci.2010.05.011.

[19] R. Shirley, Y. Liu, T. S. Totton, R. H. West, M. Kraft, First-Principles Thermochemistry for the Combustion of a $TiCl_4$ and $AlCl_3$ Mixture, J. Phys. Chem. A 113 (49) (2009) 13790–6, doi:10.1021/jp905244w.

[20] P. T. Spicer, O. Chaoul, S. Tsantilis, S. E. Pratsinis, Titania Formation by $TiCl_4$ Gas Phase Oxidation, Surface Growth and Coagulation, J. Aerosol Sci. 33 (1) (2002) 17–34, doi:10.1016/S0021-8502(01)00069-6.

[21] K. Nakaso, T. Fujimoto, T. Seto, M. Shimada, K. Okuyama, M. M. Lunden, Size Distribution Change of Titania Nano-Particle Agglomerates Generated by Gas Phase Reaction, Agglomeration, and Sintering, Aerosol Sci. Technol. 35 (5) (2001) 929–47, doi:10.1080/02786820126857.

[22] S. H. Park, S. N. Rogak, A One-Dimensional Model for Coagulation, Sintering, and Surface Growth of Aerosol Agglomerates, Aerosol Sci. Technol. 37 (12) (2003) 947–60, doi:10.1080/02786820300899.

[23] J. Akroyd, A. J. Smith, R. Shirley, L. R. McGlashan, M. Kraft, A Coupled CFD-Population Balance Approach for Nanoparticle Synthesis in Turbulent Reacting Flows, Chem. Eng. Sci. 66 (17) (2011) 3792–805, doi:10.1016/j.ces.2011.05.006.

[24] R. Shirley, J. Akroyd, L. A. Miller, O. R. Inderwildi, U. Riedel, M. Kraft, Theoretical Insights Into the Surface Growth of Rutile TiO_2, Combust. Flame 158 (10) (2011) 1868–76, doi:10.1016/j.combustflame.2011.06.007.

[25] M. Mehta, Y. Sung, V. Raman, R. O. Fox, Multiscale Modeling of TiO_2 Nanoparticle Production in Flame Reactors: Effect of Chemical Mechanism, Ind. Eng. Chem. Res. 49 (21) (2010) 10663–73, doi:10.1021/ie100560h.

[26] M. Mehta, R. O. Fox, P. Pepiot, Reduced Chemical Kinetics for the Modeling of TiO_2 Nanoparticle Synthesis in Flame Reactors, Ind. Eng. Chem. Res. 54 (20) (2015) 5407–15, doi:10.1021/acs.iecr.5b00130.

[27] A. McNaught, The IUPAC International Chemical Identifier: InChI - A New Standard for Molecular Informatics, Chem. Int. 28 (6) (2006) 12–5.

[28] International Union of Pure and Applied Chemistry, InChI: Open-Source Chemical Structure Representation Algorithm, Technical FAQ, InChI Trust, URL `http://www.inchi-trust.org/technical-faq/`, 2014.

[29] D. Weininger, SMILES, a Chemical Language and Information System. 1. Introduction to Methodology and Encoding Rules, J. Chem. Inform. Comput. Sci. 28 (1) (1988) 31–6.

[30] N. M. O'Boyle, M. Banck, C. A. James, C. Morley, T. Vandermeersch, G. R. Hutchison, Open Babel: An Open Chemical Toolbox, J. Cheminform. 3 (1) (2011) 1–14, doi:10.1186/1758-2946-3-33.

[31] D. Weininger, A. Weininger, J. L. Weininger, SMILES. 2. Algorithm for Generation of Unique SMILES Notation, J. Chem. Inform. Comput. Sci. 29 (2) (1989) 97–101, doi:10.1021/ci00062a008.

[32] P. Buerger, D. Nurkowski, J. Akroyd, S. Mosbach, M. Kraft, First-Principles Thermochemistry for the Thermal Decomposition of Titanium Tetraisopropoxide, J. Phys. Chem. A 119 (30) (2015) 8376–87, doi:10.1021/acs.jpca.5b01721.

[33] A. D. Boese, J. M. L. Martin, N. C. Handy, The Role of the Basis Set: Assessing Density Functional Theory, J. Chem. Phys. 119 (6) (2003) 3005–14, doi:10.1063/1.1589004.

[34] M. W. D. Hanson-Heine, M. W. George, N. A. Besley, Investigating the Calculation of Anharmonic Vibrational Frequencies Using Force Fields Derived from Density Functional Theory, J. Phys. Chem. A 116 (17) (2012) 4417–25, doi:10.1021/jp301670f.

[35] S. M. Tekarli, M. L. Drummond, T. G. Williams, T. R. Cundari, A. K. Wilson, Performance of Density Functional Theory for 3d Transition Metal-Containing Complexes: Utilization of the Correlation Consistent Basis Sets, J. Phys. Chem. A 113 (30) (2009) 8607–14, doi:10.1021/jp811503v.

[36] W. Jiang, M. L. Laury, M. Powell, A. K. Wilson, Comparative Study of Single and Double Hybrid Density Functionals for the Prediction of 3d Transition Metal Thermochemistry, J. Chem. Theory. Comput. 8 (11) (2012) 4102–11, doi:10.1021/ct300455e.

[37] M. L. Laury, A. K. Wilson, Performance of Density Functional Theory for Second Row (4d) Transition Metal Thermochemistry, J. Chem. Theory. Comput. 9 (9) (2013) 3939–46, doi:10.1021/ct400379z.

[38] Y. Ge, D. DePrekel, K.-T. Lam, K. Ngo, P. Vo, Assessing Density Functionals for the Prediction of Thermochemistry of $Ti-O-Cl$ Species, J. Theor. Comput. Chem. 14 (08) (2015) 1550055, doi:10.1142/S0219633615500558.

[39] J. P. Merrick, D. Moran, L. Radom, An Evaluation of Harmonic Vibrational Frequency Scale Factors, J. Phys. Chem. A 111 (45) (2007) 11683–700, doi:10.1021/jp073974n.

[40] M. J. Frisch, G. W. Trucks, H. B. Schlegel, G. E. Scuseria, M. A. Robb, J. R. Cheeseman, G. Scalmani, V. Barone, B. Mennucci, G. A. Petersson, H. Nakatsuji, M. Caricato, X. Li, H. P. Hratchian, A. F. Izmaylov, J. Bloino, G. Zheng, J. L. Sonnenberg, M. Hada, M. Ehara, K. Toyota, R. Fukuda, J. Hasegawa, M. Ishida, T. Nakajima, Y. Honda, O. Kitao, H. Nakai, T. Vreven, J. A. Montgomery, Jr., J. E. Peralta, F. Ogliaro, M. Bearpark, J. J. Heyd, E. Brothers, K. N. Kudin, V. N. Staroverov,

R. Kobayashi, J. Normand, K. Raghavachari, A. Rendell, J. C. Burant, S. S. Iyengar, J. Tomasi, M. Cossi, N. Rega, J. M. Millam, M. Klene, J. E. Knox, J. B. Cross, V. Bakken, C. Adamo, J. Jaramillo, R. Gomperts, R. E. Stratmann, O. Yazyev, A. J. Austin, R. Cammi, C. Pomelli, J. W. Ochterski, R. L. Martin, K. Morokuma, V. G. Zakrzewski, G. A. Voth, P. Salvador, J. J. Dannenberg, S. Dapprich, A. D. Daniels, Ö. Farkas, J. B. Foresman, J. V. Ortiz, J. Cioslowski, D. J. Fox, Gaussian 09 Revision D.01, 2009.

[41] D. McQuarrie, J. Simon, Molecular Thermodynamics, University Science Books, Sausalito, CA, United States, ISBN 9781891389054, 1999.

[42] J. M. Seddon, J. D. Gale, Thermodynamics and Statistical Mechanics, The Royal Society of Chemistry, Cambridge, United Kingdom, ISBN 978-0-85404-632-4, doi:10.1039/9781847552181-00077, 2001.

[43] Jmol: An Open-Source Java Viewer for Chemical Structures in 3D, URL `http://www.jmol.org/`, v14.6.4, 2016.

[44] W. J. Hehre, R. Ditchfield, L. Radom, J. A. Pople, Molecular Orbital Theory of the Electronic Structure of Organic Compounds. V. Molecular Theory of Bond Separation, J. Am. Chem. Soc. 92 (16) (1970) 4796–801, doi:10.1021/ja00719a006.

[45] J. A. Pople, L. Radom, W. J. Hehre, Molecular Orbital Theory of the Electronic Structure of Organic Compounds. VII. Systematic Study of Energies, Conformations, and Bond Interactions, J. Am. Chem. Soc. 93 (2) (1971) 289–300, doi:10.1021/ja00731a001.

[46] J. A. Pople, M. J. Frisch, B. T. Luke, J. S. Binkley, A Møller-Plesset Study of the Energies of AHn Molecules (A = Li to F), Int. J. Quantum Chem. 24 (S17) (1983) 307–20, doi:10.1002/qua.560240835.

[47] P. Buerger, J. Akroyd, J. W. Martin, M. Kraft, A Big Data Framework to

Validate Thermodynamic Data for Chemical Species, Combust. Flame 176 (2017) 584–91, doi:10.1016/j.combustflame.2016.11.006.

[48] P. Buerger, J. Akroyd, S. Mosbach, M. Kraft, A Systematic Method to Estimate and Validate Enthalpies of Formation Using Error-Cancelling Balanced Reactions, Combust. Flame, 187 (2018) 105–21, doi:10.1016/j.combustflame.2017.08.013.

[49] M. W. J. Chase Jr., NIST-JANAF Thermochemical Tables, 4th Edition, American Institute of Physics, New York, 1998.

[50] P. J. Linstrom, W. G. Mallard (Eds.), NIST Chemistry WebBook, NIST Standard Reference Database Number 69, National Institute of Standards and Technology (NIST), Gaithersburg MD, 20899, retrieved May 13, 2016, 2005.

[51] S. Abramowitz, M. Chase, Thermodynamic Properties of Gas Phase Species of Importance to Ozone Depletion, Pure Appl. Chem. 63 (10) (1991) 1449–54.

[52] R. Atkinson, D. L. Baulch, R. A. Cox, R. F. Hampson, J. A. Kerr, M. J. Rossi, J. Troe, Evaluated Kinetic and Photochemical Data for Atmospheric Chemistry, Organic Species: Supplement VII, J. Phys. Chem. Ref. Data 28 (2) (1999) 191–393, doi:10.1063/1.556048.

[53] W. J. Bloss, S. L. Nickolaisen, R. J. Salawitch, R. R. Friedl, S. P. Sander, Kinetics of the ClO Self-Reaction and 210 nm Absorption Cross Section of the ClO Dimer, J. Phys. Chem. A 105 (50) (2001) 11226–39, doi:10.1021/jp012429y.

[54] D. L. Hildenbrand, Low-Lying Electronic Sates and Revised Thermochemistry of TiCl, $TiCl_2$, and $TiCl_3$, J. Phys. Chem. A 113 (8) (2009) 1472–4, doi:10.1021/jp807913c.

[55] E. Rühl, U. Rockland, H. Baumgärtel, O. Lösking, M. Binnewies, H. Willner, Photoionization Mass Spectrometry of Chlorine Oxides, Int. J. Mass Spectrom. 185–187 (1999) 545–58, doi:10.1016/S1387-3806(98)14137-4.

[56] J. Sicre, C. Cobos, Thermochemistry of the Higher Chlorine Oxides ClO_x (x=3, 4) and Cl_2O_x (x=3-7), J. Mol. Struc.-THEOCHEM 620 (2–3) (2003) 215–26, doi:10.1016/S0166-1280(02)00602-4.

[57] W. B. DeMore, S. P. Sander, D. Golden, R. F. Hampson, M. J. Kurylo, C. Howard, A. Ravishankara, C. Kolb, M. Molina, Chemical Kinetics and Photochemical Data for Use in Stratospheric Modeling. Evaluation No. 12, J. Org. Chem. .

[58] S. L. Nickolaisen, R. R. Friedl, S. P. Sander, Kinetics and Mechanism of the Chlorine Oxide ClO + ClO Reaction: Pressure and Temperature Dependences of the Bimolecular and Termolecular Channels and Thermal Decomposition of Chlorine Peroxide, J. Phys. Chem. 98 (1) (1994) 155–69, doi:10.1021/j100052a027.

[59] T.-H. Wang, A. M. Navarrete-López, S. Li, D. A. Dixon, J. L. Gole, Hydrolysis of $TiCl_4$: Initial Steps in the Production of TiO_2, J. Phys. Chem. A 114 (28) (2010) 7561–70, doi:10.1021/jp102020h.

[60] T. J. Lee, C. M. Rohlfing, J. E. Rice, An Extensive *Ab Initio* Study of the Structures, Vibrational Spectra, Quadratic Force Fields, and Relative Energetics of Three Isomers of Cl_2O_2, J. Chem. Phys. 97 (9) (1992) 6593–605, doi:10.1063/1.463663.

[61] W.-K. Li, C.-Y. Ng, Gaussian-2 *Ab Initio* Study of Isomeric Cl_2O_2 and $Cl_2O_2{}^+$ and Their Dissociation Reactions, J. Phys. Chem. A 101 (2) (1997) 113–5, doi:10.1021/jp962253d.

[62] W.-K. Li, K.-C. Lau, C. Y. Ng, H. Baumgärtel, K. M. Weitzel, Gaussian-2 and Gaussian-3 Study of the Energetics and Structures of Cl_2O_n and

Cl_2O_n+, n = 1 − 7, J. Phys. Chem. A 104 (14) (2000) 3197–203, doi: 10.1021/jp993398y.

[63] D. G. Goodwin, An Open-Source, Extensible Software Suite for CVD Process Simulation, URL `www.cantera.org`, 2003.

[64] D. G. Goodwin, H. K. Moffat, R. L. Speth, Cantera: An Object-Oriented Software Toolkit for Chemical Kinetics, Thermodynamics, and Transport Processes, `http://www.cantera.org`, Version 2.2.1, 2016.

[65] B. J. McBride, S. Gordon, M. A. Reno, Coefficients for Calculating Thermodynamic and Transport Properties of Individual Species, Tech. Rep. NASA-TM-4513, National Aeronautics and Space Administration Washington DC, 1993.

[66] B. Karlemo, P. Koukkari, J. Paloniemi, Formation of Gaseous Intermediates in Titanium(IV) Chloride Plasma Oxidation, Plasma Chem. Plasma Process. 16 (1) (1996) 59–77, doi:10.1007/BF01465217.

[67] D. Nurkowski, P. Buerger, J. Akroyd, M. Kraft, A Detailed Kinetic Study of the Thermal Decomposition of Tetraethoxysilane, Proc. Combust. Inst. 35 (2) (2015) 2291–8, doi:10.1016/j.proci.2014.06.093.

[68] P. Buerger, D. Nurkowski, J. Akroyd, M. Kraft, A Kinetic Mechanism for the Thermal Decomposition of Titanium Tetraisopropoxide, Proc. Combust. Inst., In Press 36 (1) (2017) 1019–27, doi:10.1016/j.proci.2016.08.062.

Click here to download Supplementary Material: chem.inp

Click here to download Supplementary Material: therm_Cp_vs_T_SI_units.csv

Click here to download Supplementary Material: therm_dHf.csv

Click here to download Supplementary Material: therm_H_vs_T_SI_units.csv

Click here to download Supplementary Material: therm_S_vs_T_SI_units.csv